Retinal Cell Biology

MicroRNA-376b-3p Suppresses Choroidal Neovascularization by Regulating Glutaminolysis in Endothelial Cells

Yifan Feng,[1] Liyang Wang,[2] Chunqiong Dong,[1] Xi Yang,[1] Jing Wang,[1] Xi Zhang,[2] Yuanzhi Yuan,[1] Jinhui Dai,[1] Jinhai Huang,[3–5] and Fei Yuan[1]

[1]Department of Ophthalmology, Zhongshan Hospital, Fudan University, Shanghai, China
[2]Department of Ophthalmology, Shanghai Geriatric Medical Center, Shanghai, China
[3]Eye Institute and Department of Ophthalmology, Eye & ENT Hospital, Fudan University, Shanghai, China
[4]Key Laboratory of Myopia, Chinese Academy of Medical Sciences, Shanghai, China
[5]Shanghai Research Center of Ophthalmology and Optometry, Shanghai, China

Correspondence: Jinhui Dai, Department of Ophthalmology, Zhongshan Hospital, Fudan University, 180# Fenglin Road, Shanghai 200032, China; dai.jinhui@zs-hospital.sh.cn. Jinhai Huang, Eye Institute and Department of Ophthalmology, Eye & ENT Hospital, Fudan University, Key Laboratory of Myopia, Chinese Academy of Medical Sciences, Shanghai Research Center of Ophthalmology and Optometry; No. 19 Baoqing Road, Shanghai 200031, China; vip999vip@163.com. Fei Yuan, Department of Ophthalmology, Zhongshan Hospital, Fudan University, 180# Fenglin Road, Shanghai 200032, China; yuanfei_zs@126.com.

YF, LW, and CD contributed equally to this work.

PURPOSE. Choroidal neovascularization (CNV) is a common pathological change of various ocular diseases that causes serious damage to central vision. Accumulated evidence shows that microRNAs (miRNAs) are closely related with the regulation of endothelial metabolism, which plays crucial roles in angiogenesis. Here, we investigate the molecular mechanism underlying the regulation of endothelial glutamine metabolism by miR-376b-3p in the progression of CNV.

METHODS. Human retinal microvascular endothelial cells (HRMECs) were transfected with control or miR-376b-3p mimics, and the expression of glutaminase 1 (GLS1), a rate-limiting enzyme in glutaminolysis, was detected by real-time PCR or Western blotting. The biological function and glutamine metabolism of transfected HRMECs were measured by related kits. Luciferase reporter assays were used to validate the CCAAT/enhancer-binding protein beta (CEBPB) was a target of miR-376b-3p. Chromatin immunoprecipitation and RNA immunoprecipitation assays were performed to verify the binding of CEBPB on the promoter region of GLS1. Fundus fluorescein angiography and immunofluorescence detected the effect of miR-376b-3p agomir on rat laser-induced CNV.

RESULTS. The expression of miR-376b-3p was decreased, whereas GLS1 expression was increased in the retinal pigment epithelial–choroidal complexes of rats with CNV. HRMECs transfected with miR-376b-3p mimic showed inhibition of CEBPB, resulting in the inactivation of GLS1 transcription and glutaminolysis. Moreover, the miR-376b-3p mimic inhibited proliferation, migration and tube formation but promoted apoptosis in HRMECs, whereas these effects counteracted by α-ketoglutarate supplementation or transfection with CEBPB overexpression plasmid. Finally, the intravitreal administration of the miR-376b-3p agomir restrained CNV formation.

CONCLUSIONS. Collectively, miR-376b-3p is a suppressor of glutamine metabolism in endothelial cells that could be expected to become a therapeutic target for the treatment of CNV-related diseases.

Keywords: microRNA, glutamine metabolism, CCAAT/enhancer-binding protein beta, endothelial cells, choroidal neovascularization

Choroidal neovascularization (CNV) is usually the final pathology of approximately 50 ocular diseases,[1,2] such as neovascular age-related macular degeneration[3] and pathologic myopia,[4] that can lead to severe, irreversible loss of central vision. The outgrowth of new blood vessels from the choroidal circulation breaks through Bruch's membrane to the retinal pigment epithelium (RPE) or hides beneath the retina, resulting in edema, exudation, hemorrhage, and outer retinal dysfunction.[5,6] Although intravitreal injections of anti- VEGF are recommended as the first-line treatment for CNV, the incomplete response and potential risk of repeat administration in the long term cannot be ignored.[7,8] Therefore understanding the determinants of CNV and searching for novel molecular targets are still needed to improve antiangiogenic therapy for CNV.

Endothelial cells (ECs) are well known as major players in ocular neovascularization, including CNV.[5] A growing body of evidence indicates that EC metabolism is a driving force of angiogenesis in parallel to well-established growth factor–based (genetic) signaling.[9,10] ECs can favor glycolysis, resulting in proliferation ECs and sprouting angiogenesis by generating adenosine triphosphate rather than

Investigative Ophthalmology & Visual Science

oxidative phosphorylation.[11] Recently, glutamine metabolism (glutaminolysis) has been considered another important metabolic pathway for ECs in addition to glycolysis.[12–15] In highly proliferative ECs, glutamine serves as an anaplerotic source of nitrogen and carbons to replenish the tricarboxylic acid cycle via glutaminase 1 (GLS1)–mediated glutaminolysis to support protein and nucleotide synthesis, whereas glutamine deprivation or the blockade of GLS1 could reduce vessel sprouting in the postnatal mouse retina.[14,15] However, whether the perturbation of glutamine metabolism in ECs alleviates CNV growth has not been thoroughly clarified.

MicroRNAs (miRNAs) constitute a class of noncoding, single-stranded RNAs with a length of approximately 22 nucleotides that can modulate the expression of target genes by binding sequences at the 3′-untranslated region (3′-UTR) of corresponding messenger RNAs (mRNAs), resulting in mRNA degradation or translational inhibition.[16,17] Recent studies in animals and humans have revealed the important functions of miRNAs in the development and progression of CNV.[18–20] We previously reported the expression profile of miRNAs in a rat model of laser-induced CNV, and in total, 29 downregulated miRNAs were identified in CNV tissues with a cutoff of a 1.5-fold change and a *P* value < 0.05.[21] Among those identified by our study, miR-376b-3p attracted our attention because it has been reported to be involved in angiogenesis after cerebral ischemia.[22] However, the exact role of miR-376b-3p in the development of CNV remains to be elucidated.

In this study, we revealed that the overexpression of miR-376b-3p can inhibit glutamine catabolism and the proliferation, migration, survival and tube formation of ECs by inhibiting GLS1 expression. Moreover, we identified CCAAT/enhancer binding protein beta (CEBPB) as a target of miR-376b-3p, and CEBPB bound the promoter region of GLS1 and activated GLS1 by transcription, thereby increasing the expression level of GLS1. These findings illustrate a new regulatory mechanism in the development of CNV-associated diseases and could provide theoretical support for future studies.

MATERIALS AND METHODS

Cell Culture

Primary human retinal microvascular endothelial cells (HRMECs) were purchased from Cell Systems (Kirkland, WA, USA) and cultured in endothelial cell medium supplemented with 5% fetal bovine serum, 1% endothelial cell growth supplement, and 1% penicillin/streptomycin solution (ScienCell Research Laboratories, Carlsbad, CA, USA) in an incubator with 5% CO_2 at 37°C. Cells at passages 3–8 were used for all experiments.

Cell Transfection

The hsa-miR-376b-3p mimic and the corresponding mimic negative control (miR-NC) oligonucleotides were purchased from RiboBio Co., Ltd. (Guangzhou, China; cat. no. miR10002172-1-5 and miR1N0000001-1-5). Small interfering RNA targeting the CEBPB gene, the pIRES2 vector with CEBPB cDNA but without miR-376b-3p targeting sites in the 3′-UTR (PIRES2_CEBPB), and the corresponding negative controls (si-NC and PIRES2_Ctrl) were synthesized by GenePharma (Shanghai, China). These constructs and

oligonucleotides were transfected into HRMECs by using Lipofectamine 3000 (Invitrogen, Carlsbad, CA, USA) according to the manufacturer's instructions. Certain experiments were performed 48 hours after the transfection as described in detail in the following sections. The sequences of the siRNAs were present in Supplementary Table S1.

Cell Proliferation Assay

Cell proliferation was quantified using Ki67 immunostaining. Briefly, HRMECs with different transfection factors were fixed in 4% paraformaldehyde (PFA; Beyotime, Jiangsu, China), followed by permeabilization with 0.2% Triton-X in PBS (Beyotime). After blocking with 10% goat serum for 30 minutes, the cells were incubated with a mouse anti-Ki67 antibody (Boster Biological Technology Co., Ltd., Wuhan, China) overnight at 4°C, followed by incubation with goat anti-mouse IgG-Alexa 594 (Jackson ImmunoResearch Laboratories, Inc., West Grove, PA, USA) for one hour at room temperature. The cells were observed in six randomly selected fields under a fluorescence microscope (BX63; Olympus, Tokyo, Japan) after nuclear staining with 4′,6-diamidino-2-phenylindole (Sigma-Aldrich, St. Louis, MO, USA), and the ratio of Ki67-positive cells to the number of total cells was calculated.

Cell Apoptosis Assay

The number of apoptotic cells was quantified using a transferase-mediated deoxyuridine triphosphate-biotin nick end-labeling (TUNEL) apoptosis assay kit (Roche, Basel, Switzerland). Briefly, HRMECs with different transfection factors were fixed with 4% PFA for 30 minutes at room temperature, washed twice with PBS, and permeabilized with 0.2% Triton X-100 for five minutes. Subsequently, the cells were subjected to TUNEL staining for one hour at room temperature in the dark, followed by 4′,6-diamidino-2-phenylindole staining for the detection of the cell nuclei. Images were acquired under a fluorescence microscope from six randomly selected fields in each well. The ratio of the number of TUNEL-positive cells to the number of total cells was calculated.

Cell Migration Assay

The cell migration ability was tested using 24-well Transwell units. In brief, HRMECs with different transfection factors were seeded into the upper well for 24 hours and allowed to invade the Transwell plate (0.4 µm pore; Corning Costar, Cambridge, MA, USA). The migrated cells on the inserts were fixed with 4% PFA, stained with crystal violet (Beyotime), and observed under a light microscope (Olympus).

Tube Formation Assay

The tube formation assay was conducted as previously described.[21] Briefly, aliquots (150 µl) of Matrigel (BD Bioscience, Franklin Lakes, NJ, USA) were added to a 48-well plate and incubated at 37°C for 30 minutes. The HRMECs were resuspended in supernatants collected from each pretreatment and then seeded onto the gel (2×10^4 cells/well). Five random fields from each well were chosen and photographed after eight hours. Networks of tube-like structures were measured using Image Pro-Plus (IPP) 6.0 software (Media Cybernetics, Rockville, MD, USA).

Glutamine Consumption, Glutamate and α-KG Measurements

HRMECs with different transfection factors were cultured in endothelial cell medium with 2 mM glutamine for 24 hours. Glutamine consumption and the cellular glutamate and α-ketoglutarate contents were determined using the respective assay kits (Abcam, Cambridge, MA, USA) according to the manufacturer's recommendations. The measurements were performed and recorded by a microplate reader (Thermo Fisher Scientific Inc., Waltham, MA, USA). The data are presented as a percentage of the control group.

Metabolic Measurements

A Seahorse XFe 96 Extracellular Flux Analyzer (Seahorse Bioscience, Billerica, MA, USA) was used to determine the oxygen consumption rate according to the manufacturer's instructions. In brief, HRMECs (1×10^4 cells/well) were seeded into a Seahorse XF 96 cell culture plate and maintained in nonbuffered assay medium in an incubator without CO_2 for one hour before the assay. The oxygen consumption rate was measured under basal conditions and after the addition of mitochondrial respiration inhibitors, including oligomycin (1 μM), carbonylcyanide-4-trifluoromethoxy-phenylhydrazone (1 μM) and rotenone (0.5 μM)/antimycin A (0.5 μM).

Reverse Transcription–Quantitative PCR (RT-qPCR)

The total RNA was isolated from HRMECs or mouse RPE/choroid/sclera complexes by using a miRNeasy Mini Kit (Qiagen, Hilden, Germany). For the mRNA detection, RNA was reverse transcribed into cDNA with a PrimeScript RT Master Mix kit (Takara, Otsu, Japan). Quantitative PCR was conducted using an ABI PRISM 7500 fast real-time PCR System (Applied Biosystems, Foster City, CA, USA) with a SYBR Premix Ex TaqTM II Kit (Takara) according to the manufacturer's instructions. For the miRNA detection, total cDNA was synthesized by using a miScript II RT kit (Qiagen) and amplified using a miScript SYBR Green PCR Kit (Qiagen). U6 small nuclear RNA and β-actin were used as internal controls for the miRNA and mRNA assays, respectively. Gene expression was calculated using the $2^{-\Delta\Delta Ct}$ method after normalization to the endogenous reference.[23] The sequences of the specific primers are presented in Supplementary Table S2.

Western Blot Analysis

The total protein was extracted from HRMECs or RPE/choroid complexes using RIPA lysis buffer containing 1% protease inhibitor and phenylmethanesulfonyl fluoride (Beyotime). After centrifugation of the lysates at 12,000g for 15 minutes at 4°C, the supernatant (total protein) was collected and quantified using a BCA assay kit (Beyotime). Equal amounts of protein from each sample were incubated with loading buffer (Beyotime) for five minutes at 95°C, separated by 10% SDS-PAGE and subsequently transferred onto polyvinylidene fluoride membranes (Millipore, Bedford, MA, USA). The membranes were blocked with 5% skimmed milk (Sigma-Aldrich) in TBS-0.05% Tween-20 (TBST) buffer (Sangon Biotech Co., Ltd., Shanghai, China) at room temperature for two hours and then incubated

with primary antibodies against GLS1 (Proteintech, Rosemont, IL, USA; cat. no. 12855-1-AP), GLS2 (Abcam; cat. no. ab150474), CEBPB (Abcam; cat. no. ab53138) and β-actin (Cell Signaling Technology, Danvers, MA, USA; cat. no. 13E5) at 4°C overnight. After the primary antibody incubation, the membranes were reacted with the secondary antibody (Cell Signaling Technology; cat. no. 7074) for one hour. The reactive bands were detected and observed via an enhanced chemiluminescence kit (Thermo Fisher Scientific Inc.). The densitometric quantification of the bands was performed with ImageJ software (National Institutes of Health) using β-actin as an internal reference.

Luciferase Reporter Assay

The wild-type (WT) and mutant-type sequences of the CEBPB-3' UTR were synthesized by GenePharma (Shanghai, China) and inserted into the pmirGLO Dual Luciferase miRNA target expression vector (Promega, Madison, WI, USA). Using Lipofectamine 3000 transfection reagent, 3'UTR-WT or -mutant-type of the CEBPB plasmid and miR-376b-3p mimic or miR-NC were cotransfected into HRMECs with 70% confluence. The cells were harvested 48 hours after the transfection, and the luciferase activities were measured by using a Luciferase Reporter Assay System (Promega) following the manufacturer's instructions. Firefly luciferase activity was normalized to that of Renilla luciferase.

Chromatin Immunoprecipitation (ChIP)

ChIP assays were carried out using an EZ- Magna ChIP A kit (Millipore; cat. no. 17–408) according to the manufacturer's protocol. The sample was lysed with lysis buffer and treated with ultrasound scanning and centrifugation. Precleared chromatin was incubated with the CEBPB antibody (Santa Cruz Biotechnology, Santa Cruz, CA, USA; cat. no. sc-7962) or normal rabbit IgG (provided with the ChIP kit) antibody overnight at 4°C. Purified DNA from the samples and the input controls were analyzed to detect the presence of GLS1 promoter sequences containing putative CEBPB response elements using RT–qPCR. The primers for the PFKFB3 promoter containing putative CEBPB binding sites were present in Supplementary Table S3.

RNA Immunoprecipitation (RIP) Assay

The relationship between miR-376b-3p and CEBPB was measured by a Magna RIP Quad RNA-binding protein immunoprecipitation kit (Millipore; cat. no. 17-704) following the manufacturer's instructions. In brief, HRMECs (2×10^6) were collected, resuspended in RIP lysis buffer containing magnetic beads, and then incubated with an anti-Argonaute 2 (Ago2) antibody (Millipore) or normal mouse IgG (Millipore) as a negative control. Subsequently, the protein was digested using proteinase K buffer, followed by RNA purification. Finally, the coprecipitated RNA was isolated and analyzed by RT–qPCR to verify the existence of the binding targets.

Animals

Adult male Brown-Norway pigmented rats weighing 175–200 g at six to eight weeks of age were purchased from SLAC Laboratory Animal (Shanghai, China). All animal protocols were approved by the Ethical Committee on Animal

Experiments of Animal Care Committee of Zhongshan Hospital, Fudan University (No. 2019-285). The animals were handled in accordance with the Association for Research in Vision and Ophthalmology (ARVO) Statement for the Use of Animals in Ophthalmic and Vision Research. The animals were allowed to acclimatize for at least seven days before the experimental manipulations.

Laser-Induced CNV Model Establishment and Treatment

CNV was induced by photocoagulation and evaluated as previously described.[21,24] In brief, rats were anesthetized with 2% sodium pentobarbital (50 mg/kg; Sigma–Aldrich), and the pupils of both eyes were dilated with 1% tropicamide (Alcon Laboratories, Fort Worth, TX, USA). Laser photocoagulation (Visulas 532s; Carl Zeiss Meditec, Jena, Germany) was performed bilaterally in each rat. Eight laser spots were applied around the optic nerve by using a slit lamp delivery system and a coverslip as a contact lens. The laser beam had a diameter of 100 μm, duration of 100 ms, and energy of 150 mW. All laser burns had the appearance of a cavitation bubble, and the spots that contained hemorrhage and those that failed to develop a bubble at the laser site were excluded from the analysis. Agomirs are chemically modified double-stranded miRNA mimics that are especially suitable for in vivo experiments because they have high stability and membrane permeability. For the miRNA treatment, the laser-treated eye received an intravitreal injection of 10 μl of PBS, agomiR-NC (0.5 nmol/μl; cat. no. miR4N0000001-4-5) or agomiR-376b-3p (0.5 nmol/μl; cat. no. miR40003196-4-5) on day 1 after the photocoagulation according to established protocols.[21,24] The rats were euthanized by intraperitoneal injection of an overdose of 2% sodium pentobarbital (200 mg/kg)[25] on day 7 for the choroidal flatmount, RT-qPCR, and Western blot analyses.

Fundus Fluorescein Angiography (FFA)

To determine CNV leakage FFA in mice were performed at baseline and 1 week after laser photocoagulation. The rats were anesthetized, and 10% fluorescein sodium (0.1 ml/kg, Fluorescite; Alcon) was injected by peritoneal injection. Consecutive recording of the ocular fundus was performed by a commercial camera and imaging system (TRC-50DX and IMAGEnet ver. 1.53; Topcon, Tokyo, Japan) with a 20-D lens in contact with the fundus camera lens. A blinded assessment of fluorescein angiogram images was conducted by two independent observers (Y.F., Y.Y.) according to previously established criteria[26]: 0, no leakage; 1, slight leakage; 2, moderate leakage; 3, prominent leakage. FFA data are expressed as the incidence of CNV angiographic grades of the total laser impacts in each group.

RPE-Choroid Flat-Mounts

Seven days after the laser photocoagulation, the rats were sacrificed, and the eyes were processed for fluorescent-labeled isolectin staining of the CNV lesions. In brief, after fixation with 4% PFA and incubation with a blocking solution that contained 0.5% bovine serum albumin and 0.2% Triton X-100 in PBS, eyecups were stained with FITC-conjugated Bandeiraea simplicifolia isolectin B4 (IB4; 1:100; Sigma-Aldrich) in blocking buffer at 4°C overnight. Using four to

six relaxing radial cuts, the RPE/choroid/sclera complex was mounted flat on a glass slide with the RPE side upward. All flat-mounts were examined and photographed under a confocal laser scanning microscope (FV3000; Olympus), and the fluorescent size was calculated using IPP 6.0 software. The average CNV size per lesion per eye was calculated. All measurements were performed by two different observers in a blinded fashion (Y.F., Y.Y.).

Statistical Analysis

Statistical analysis commercial software was used for the statistical analysis (SPSS 21.0; SPSS, Chicago, IL, USA). Each experiment was repeated at least three times. The data are expressed as the means $\pm$ SEM. Comparisons between two groups were performed by using Student's *t*-tests, and comparisons among >2 groups were performed by using a one-way ANOVA, followed by Bonferroni's post-hoc test. Values of $P < 0.05$ were considered statistically significant.

RESULTS

Ectopic miR-376b-3p Expression Blocked Glutaminolysis in HRMECs

Based on the results of our previous miRNA expression profiling,[21] nine miRNAs, including miR-376b-3p, were found to be significantly downregulated in CNV tissues with a cutoff value $\geq$ 2-fold and a P value < 0.5 (Supplementary Fig. S1A). MiR-376b-3p belongs to the miR-376 family, which includes miR-376a, miR-376b, and miR-376c, all located within the 14q32 locus.[27] Moreover, hsa-miR-376b was found to be highly homologous to other vertebrates, such as 99% homology with rhesus monkeys (Macaca mulatta) and 94% homology with mice (Mus musculus) and rats (Rattus norvegicus) in the microRNAviewer (http://people.csail.mit.edu/akiezun/miRviewer) (Supplementary Fig. S1B).[28] Furthermore, RT–qPCR was performed to identify the expression levels of miR-376b-3p and GLS1 in normal and CNV tissues. As shown in Figures 1A and 1B, compared with normal tissues, the level of miR-376b-3p in CNV tissues was significantly reduced. Conversely, the mRNA level of GLS1 in the CNV tissues was markedly higher than that in the normal tissues.

ECs are recognized as major players in ocular angiogenesis.[29] To verify whether miR-376b-3p indeed regulates glutaminolysis, HRMECs were transfected with a miR-376b-3p mimic or NC mimic, and the mRNA expression of miR-376b-3p was confirmed by RT–qPCR (Fig. 1C). The overexpression of miR-376b-3p inhibited both the mRNA and protein levels of GLS1, but not GLS2, in HRMECs (Figs. 1D–F). As expected, the miR-376b-3p mimic observably inhibited glutamine consumption and decreased the cellular glutamate and α-KG levels in HRMECs (Figs. 1G–I). Meanwhile, the rate of oxygen consumption was also suppressed in the miR-376b-3p mimic transfection group (Figs. 1J, 1K). Taken together, these results demonstrate that miR-376b-3p suppresses cell glutaminolysis in HRMECs.

Ectopic miR-376b-3p Expression Suppressed The Biological Function of HRMECs

Given that GLS1-mediated glutaminolysis plays a crucial role in regulating EC biology,[12,14,15] we further investigated the regulatory effects of miR-376b-3p on EC function in
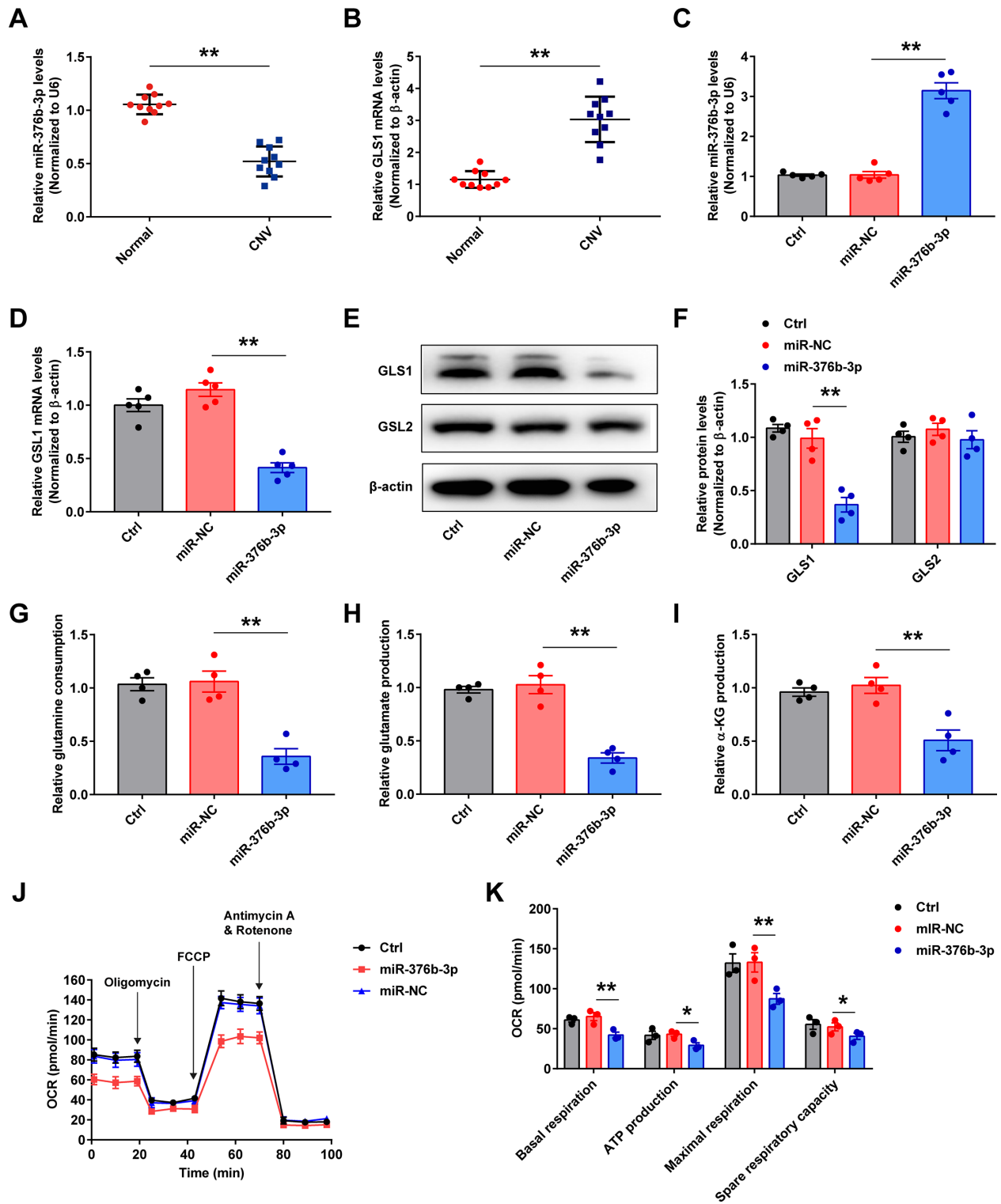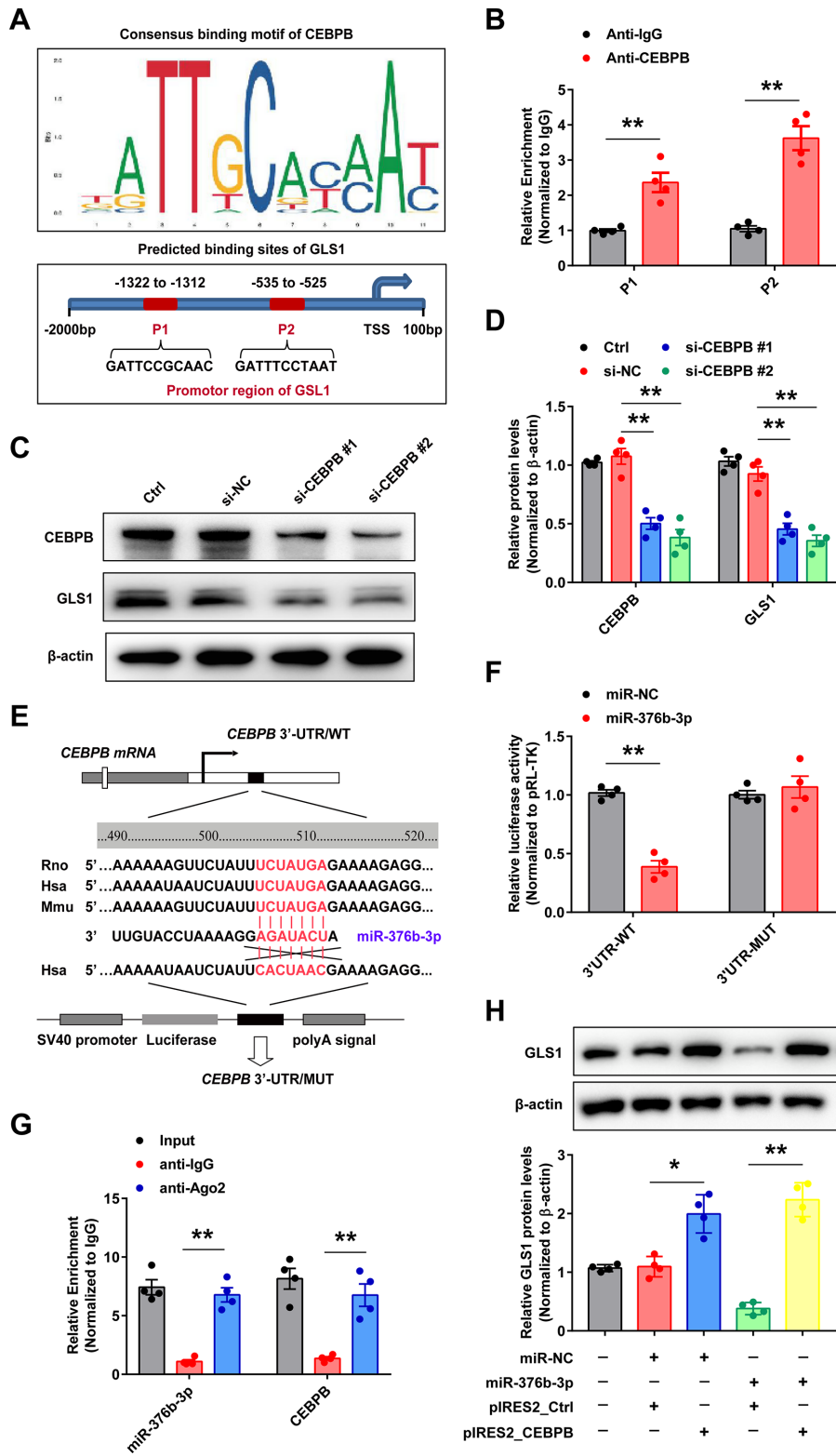
FIGURE 1. Ectopic miR-376b-3p expression blocked glutaminolysis in HRMECs. (**A, B**) RT-qPCRs were performed to detect the expression of miR-376b-3p and GLS1 in the RPE/choroid complexes of Brown-Norway rats on day 7 after photocoagulation. (**C, D**) RT-qPCRs were performed to detect the expression of miR-376b-3p and GLS1 in HRMECs transfected with miR-376b-3p mimic or miR-NC. (**E, F**) Representative Western blot and quantitative analysis of GLS1 and GLS2 in transfected HRMECs. (**G–I**) The levels of glutamine consumption, cellular glutamate and α-KG in transfected HRMECs were measured by indicated kits. (**J**) Mitochondrial mito-stress assay in HRMECs after treatment by seahorse, cells were challenged with oligomycin (1 µM), carbonylcyanide-4-trifluoromethoxy-phenylhydrazone (0.5 µM) and RO/AA (0.5 µM). (**K**) Quantification of basal respiration, adenosine triphosphate concentration, maximal respiration and spare respiration capacity in HRMECs. Each experiment repeated more than three times, and data in graphs represent the mean ± SEM. *$P < 0.05$; **$P < 0.01$.
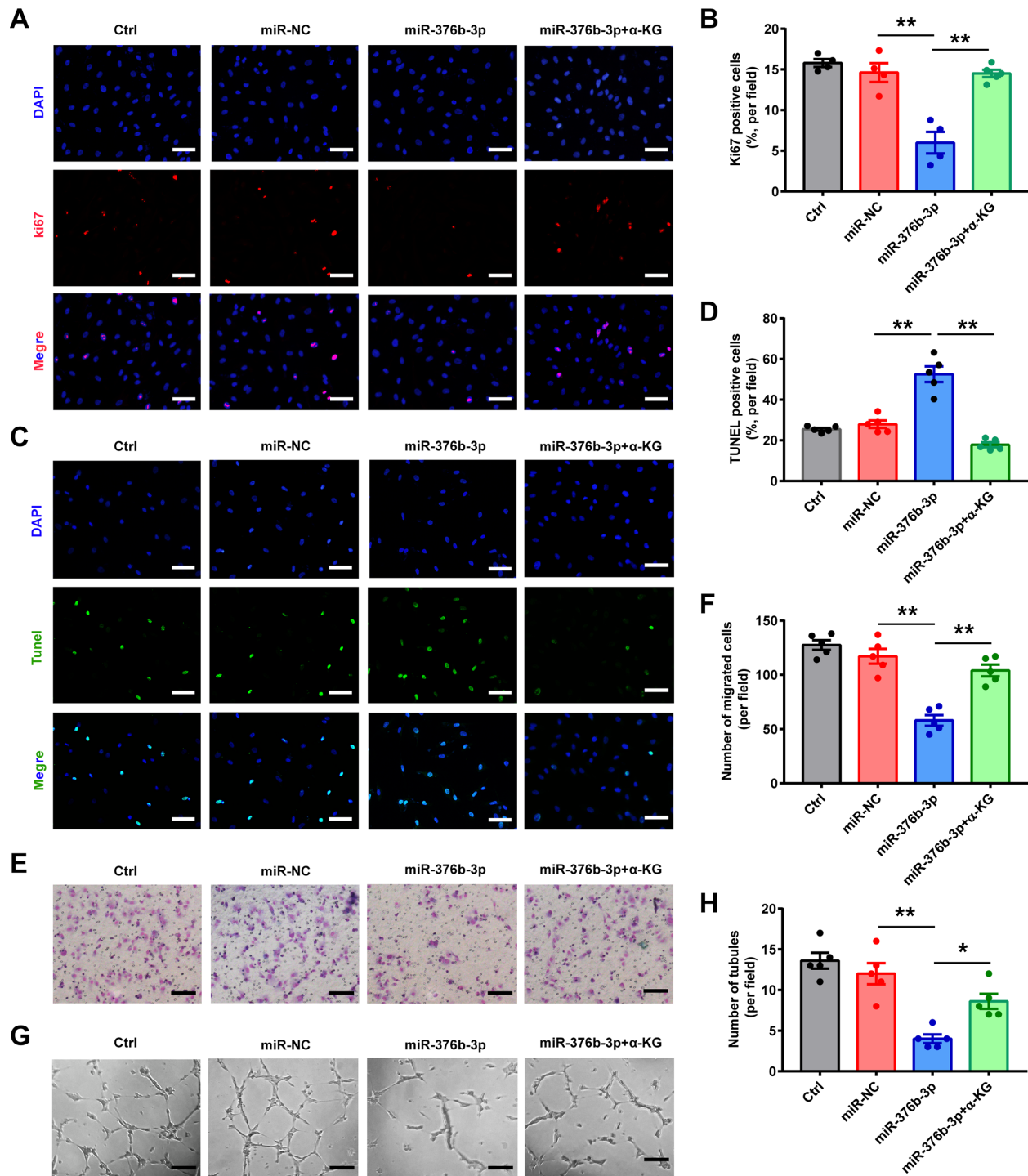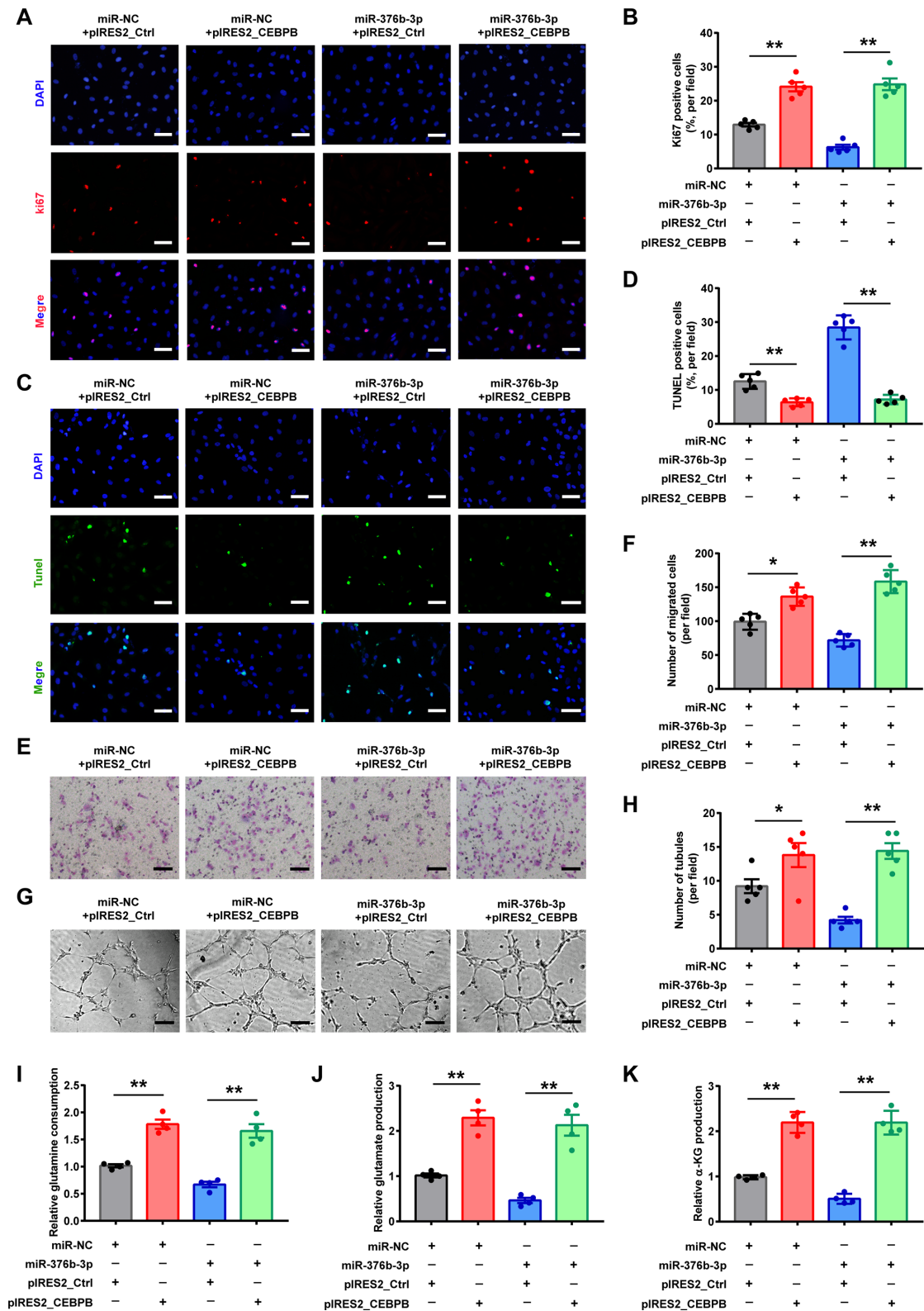
FIGURE 2. Ectopic miR-376b-3p expression suppressed the biological function of HRMECs. (**A, B**) Ki67 (*red*) immunofluorescence staining were performed to determine the number cell proliferation in HRMECs transfected with miR-376b-3p mimic or miR-NC, or miR-376b-3p mimic plus α-KG supplementation (100 mM). *Scale bar:* 50 µm. (**C, D**) TUNEL (*green*) assay were performed to detect the number of cell apoptosis in HRMECs from the indicated groups. *Scale bar:* 50 µm. (**E, F**) Transwell assay were performed to assess the migration of HRMECs from the indicated groups and the cells migrated through the chamber in 5 randomly selected fields were quantified at 24 h after cell seeding. *Scale bar:* 100 µm. (**G, H**) HRMECs from the indicated groups were seeded on the Matrigel matrix. The quantification of tube-like structures was analyzed at 8 h after cell seeding. *Scale bar:* 100 µm. Each experiment repeated more than three times, and data in graphs represent the mean ± SEM. *$P < 0.05$; **$P < 0.01$.

vitro. The results of the Ki67 and TUNEL staining demonstrated that the overexpression of miR-376b-3p remarkably suppressed cell proliferation (2A, B) but increased the

number of apoptotic cells (Figs. 2C, 2D). Moreover, in the Transwell assays, the cells treated with the miR-376b-3p mimic showed an ~45% reduction in migration compared

FIGURE 3. Ectopic miR-376b-3p regulates GLS1 expression by targeting CEBPB. (**A**) Consensus binding motif of CEBPB and the binding sites of CEBPB on the promoter of GLS1 were predicted using JASPAR database. (**B**) Binding of CEBPB to the GLS1 promoter region in HRMECs was detected by ChIP assay. (**C, D**) Representative Western blot and quantitative analysis of GLS1 in HRMECs transfected with small interfering RNA targeting the CEBPB gene or si-NC. (**E**) Diagram of putative miR-376b-3p binding sites in 3′-UTR of CEBPB and GLS1. Red portions of sequences represent the WT and MUT binding sites of miR-376b-3p in GLS1 3′-UTR. (**F**) The luciferase activity of GLS1-3′-UTR reporter plasmids treated with miR-376b-3p mimic or miR-NC mimics determined by dual-luciferase reporter assay. (**G**) RIP assay was used for detection of the enrichment of miR-376b-3p and CEBPB in response to anti-Ago2 compare to the negative control IgG. (**H**) Representative Western blot and quantitive analysis of GLS1 in HRMECs transfected with miR-376b-3p or miR-NC mimics, or the miR-376b-3p mimic plus the CEBPB expression plasmid (pIRES2_CEBPB) or negative control plasmid (pIRES2_Ctrl). Each experiment repeated more than three times, and data in graphs represent the mean ± SEM. *$P < 0.05$; **$P < 0.01$.

FIGURE 4. CEBPB reverses the suppressive effects of miR-376b-3p in HRMECs. (**A, B**) Ki67 (*red*) immunofluorescence staining were performed to determine the number cell proliferation in HRMECs transfected with miR-376b-3p or miR-NC mimics plus the CEBPB expression plasmid (pIRES2_CEBPB) or negative control plasmid (pIRES2_Ctrl). *Scale bar:* 50 µm. (**C, D**) TUNEL (*green*) assay were performed to detect the number of cell apoptosis in HRMECs from the indicated groups. *Scale bar:* 50 µm. (**E, F**) Transwell assay were performed to assess the migration of HRMECs from the indicated groups and the cells migrated through the chamber in 5 randomly selected fields were quantified at 24 hours after cell seeding. *Scale bar:* 100 µm. (**G, H**) HRMECs from the indicated groups were seeded on the Matrigel matrix. The quantification of tube-like structures was analyzed at 8 h after cell seeding. *Scale bar:* 100 µm. (**I–K**) The levels of glutamine consumption, cellular glutamate and α-KG in transfected HRMECs were measured by indicated kits. Each experiment repeated three times, and data in graphs represent the mean ± SEM. *$P < 0.05$; **$P < 0.01$.
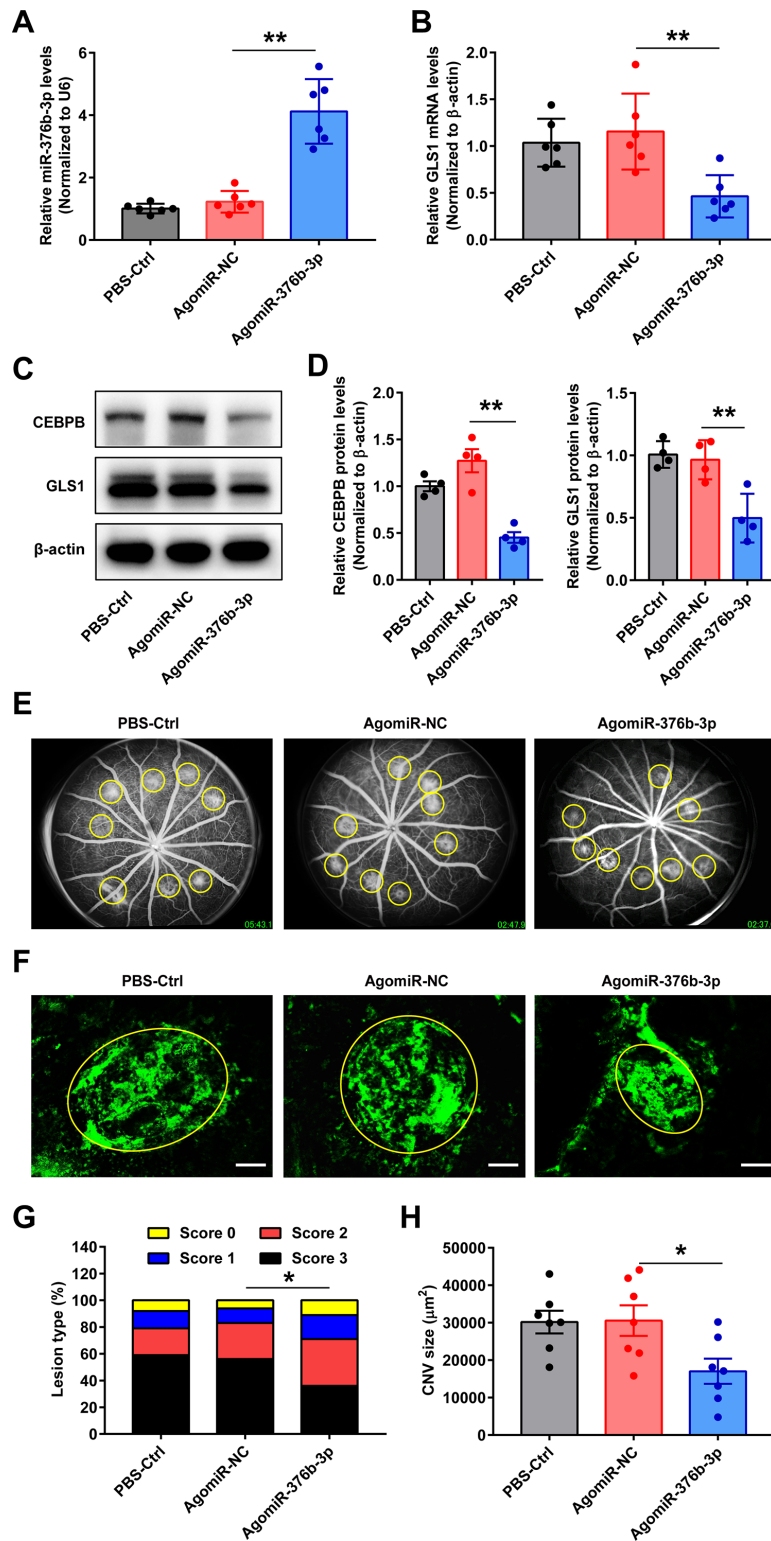
FIGURE 5. Intravitreal injection of miR-376b-3p represses laser-induced CNV in rats. (**A, B**) RT-qPCR analysis showing the up-regulation of miR-376b-3p and down-regulation of GLS1 by miR-376b-3p mimic injection in the Brown-Norway rat eyes at 7 days after photocoagulation. PBS and miR-NC injections were used as controls. The miRNA and mRNA levels were normalized to U6 and β-actin. (**C, D**) Representative Western blot and quantitative analysis of CEBPB and GLS1 in RPE/choroid/sclera complexes from the indicated groups. The β-actin served as an endogenous reference for normalization. (**E, G**) Representative images of choroidal vascular leakage on fundus fluorescein angiography (FFA) from the indicated groups. Data are expressed as the incidence of CNV angiographic grades of the total laser impacts in each group. n = 6 rats /group for all experiments. (**F, H**) Representative images of choroidal flatmounts and quantitative analysis of CNV size from the indicated groups. CNV sizes are expressed as mean ± SEM of the average CNV size per rat. n = 7 rats /group for all experiments. *Scale bar:* 50 μm. The margins of the CNV lesion are outlined by solid yellow lines. Each experiment repeated more than three times, and data in graphs represent the mean ± SEM. $^{*}P < 0.05$, $^{**}P < 0.01$.

with the NC mimic group (Figs. 2E, 2F). In addition, miR-376b-3p substantially suppressed the tube formation of HRMECs, resulting in reductions of ~75% in mesh numbers (Figs. 2G, 2H). However, the supplementation with exogenous α-KG reversed all biological properties of the miR-376b-3p-transfected HRMECs (Figs. 2A–H). Overall, these data reveal that miR-376b-3p inhibits the angiogenic function of HRMECs depending on glutaminolysis inhibition.

Ectopic miR-376b-3p Regulates GLS1 Expression by Targeting CEBPB

To understand the mechanism by which miR-376b-3p regulates the expression of GLS1, we examined the possibility that miR-376b-3p could bind the 3′-UTR of GLS1. However, the analysis using TargetScan and the miRDB prediction tool resulted in no miR-376b-3p binding sites in the 3′-UTR of GLS1 (data not shown), suggesting that miR-376b-3p indirectly regulates GLS1 expression. Therefore, we hypothesized that a transcription factor regulating the gene encoding GLS1 might be targeted by miR-376b-3p. By searching the bioinformatics databases JASPAR (http://jaspar.genereg.net/)[30] and Eukaryotic Promoter Database (EPD, http://epd.vital-it.ch/),[31] we noticed that CEBPB harbors a putative binding site for GLS1 (Fig. 3A). The ChIP experiments showed that CEBPB tightly bound the transcribed regions (P1 and P2) of the GLS1 gene (Fig. 3B). In addition, the knockdown of CEBPB remarkably reduced the expression of both CEBPB and GLS1 at the protein level (Figs. 3C, 3D). These results suggest that CEBPB transcription activates GLS1 in HRMECs.

To further confirm that CEBPB is a direct target of miR-376b–3p, we used the biological software TargetScan (http://www.targetscan.org/)[32] and miRDB (http://mirdb.org)[33] to predict the binding sites between miR-376b-3p and the 3′-UTR regions of CEBPB. As shown in Figure 3E, a conserved sequence in the 3′-UTR of CEBPB was predicted as the binding sequence of miR-376b-3p. Subsequently, we constructed luciferase reporter vectors containing the wild-type and mutant binding sites of the GLS1 3′-UTR, and the results showed that the overexpression of miR-376b-3p led to a marked decrease in the luciferase activity of the wild-type 3′-UTR plasmid, but no significant change was observed with the mutant vector (Fig. 3F). Concurrently, the RIP analysis showed that miR-376b-3p and CEBPB were both enriched in Ago2-coated beads relative to the IgG control group (Fig. 3G). The Western blot analysis also showed that CEBPB overexpression could reverse the expression of the GLS1 protein in the HRMECs transfected with the miR-376b-3p mimics (Fig. 3H). Collectively, these experimental results reveal that miR-376b-3p regulates the expression of GLS1 by targeting CEBPB.

CEBPB Reverses The Suppressive Effects of miR-376b-3p in HRMECs

To further validate the role of CEBPB in miR-376b-3p-mediated biofunctions, HRMECs were cotransfected with an NC mimic or miR-376b-3p mimic and empty plasmid or CEBPB-expressing plasmid. As expected, the concomitant overexpression of CEBPB largely abrogated the suppressive effects of miR-376b-3p on cell proliferation, survival, migration and tube formation (Figs. 4A–H). We further investigated the role of CEBPB in miR-376b-3p-induced glutaminolysis inhibition in HRMECs, and the results revealed that miR-376b-3p inhibited glutamine consumption and glutamate and α-KG production, which was antagonized by the overexpression of CEBPB (Figs. 4I–K). These results demonstrate that miR-376b-3p inhibits the glutaminolysis and angiogenesis of HRMECs by targeting CEBPB.

Intravitreal Injection of miR-376b-3p Represses Laser-Induced CNV in Rats

Finally, we examined the effect of miR-376b-3p on laser-induced CNV in rats. An intravitreal injection of PBS, a miR-376b-3p mimic or an NC mimic was administered immediately after laser injury. Eyes were collected at seven days after the laser injury for RT–qPCR, FFA and confocal imaging assays. The RT-qPCR results confirmed that the injection of the miR-376b-3p mimic led to an increase in miR-376b-3p expression (Figs. 5A, 5B) but a decrease in CEBPB and GLS1 expression in the RPE/choroid/sclera complex (Figs. 5C, 5D). Additionally, compared with CNV lesions in the PBS- or NC mimic-treated control groups, CNV lesions in the miR-376b-3p -treated group showed reduced choroidal vascular leakage (Figs. 5E, 5G). Similarly, the confocal images of RPE/choroid flat mounts stained with IB4 revealed that the average lesion size in the eyes treated with the miR-376b-3p mimic was significantly smaller than that observed
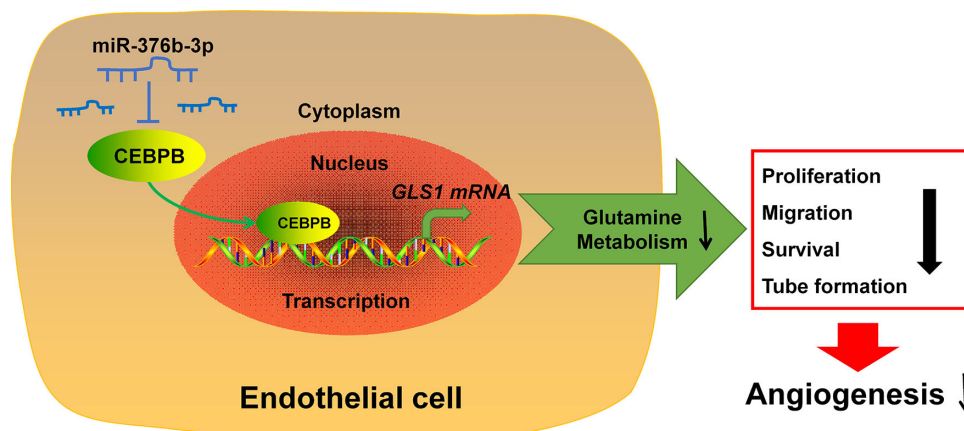

FIGURE 6. Schematic of miR-376b-3p impact on choroidal neovascularization in rat laser burn model.

in the PBS- or NC mimic-treated control eyes (Figs. 5F, 5H). Collectively, these results suggest that the therapeutic delivery of miR-376b-3p prevents the development of CNV (Fig. 6).

DISCUSSION

CNV is a pathological process in which aberrant blood vessels rupture Bruch's membrane and invade the pigment epithelium or subretinal space. Multiple mechanisms, such as hypoxia, inflammation and imbalance of angiogenic and antiangiogenic factors, have been proposed to initiate CNV growth.[5,34] Mounting evidence indicates that miRNA-based therapy may provide a rational basis for effective anti-CNV treatment.[18,20] MiR-376b-3p is highly conserved among vertebrates and has been shown to be downregulated in a variety of cancers.[35–37] Notably, the overexpression of miR-376b-3p could inhibit cell proliferation, survival and migration, affecting the development of tumors.[35,36,38,39] However, the possible regulatory function of miR-376b-3p in other types of cells, especially in EC, remains unclear and urgent to be elucidated.

In this study, we first demonstrated that the expression of miR-376b-3p was downregulated, whereas GLS1 expression was upregulated in laser-induced CNV in Brown-Norway rats. Moreover, HRMECs transfected with a miR-376b-3p mimic showed inhibition of the mRNA and protein levels of CEBPB, a member of the transcription factor family of CEBP, to promote GLS1 transcription, resulting in the activation of glutaminolysis. In addition, the upregulation of miR-376b-3p inhibited proliferation, migration and tube formation but promoted apoptosis in ECs. Finally, the intravitreal administration of exogenous miR-376b-3p reversed the increased mRNA and protein levels of CEBPB and GLS1 in the choroidal tissue after laser injury and restrained CNV formation. These results suggest that miR-376b-3p is a therapeutic target for CNV treatments.

Glutamine is a major source of carbon and energy to promote EC growth and viability.[40] GLS1 serves as a first and rate-limiting glutaminolysis enzyme that catalyzes the conversion of glutamine into glutamate, which is further metabolized to α-KG, a key intermediate in tricarboxylic acid. A previous in vitro study revealed that glutamine deprivation or the pharmacological inhibition of GLS1 blocked endothelial proliferation, migration, viability and cell cycle progression regardless of the vascular source.[12] Moreover, the blockage of glutaminolysis in ECs induced senescence.[41] In vivo studies further showed that the endothelial-specific deletion of GLS1 in mice markedly restrained vessel sprouting.[14,15] More recently, we reported that the systemic administration of the GLS1 inhibitor CB-839 significantly reduced corneal neovascularization in mice.[42] Altogether, these findings indicate that GLS1 is a promising therapeutic target for treating CNV. Notably, we observed that the expression of GLS1 increased in the rat retinas in the CNV group compared with that in the normal retinas. Although the combination of TargetScan and miRDB software did not predict that GLS1 is a putative target gene of miR-376b-3p, an inverse correlation between the levels of miR-376b-3p and GLS1 was detected in HRMECs. Consistent with this observation, we also found that GLS1-mediated glutaminolysis was significantly downregulated by the overexpression of miR-376b-3p in HRMECs.

CEBPB, also known as nuclear factor-IL6, is a member of the CEBP transcription factor family that contains basic leucine zipper and regulates the transcription of target genes by binding DNA-binding sites (consensus sequence "CCAAT").[43] Abundant evidence confirms that CEBPB participates in differentiation, inflammation, apoptosis and metabolism in various cells.[44,45] Importantly, CEBPB has also been reported to be responsible for pathological angiogenesis. For instance, Zhang et al.[46] reported that CEBPB plays a critical role in M2 macrophage polarization and facilitates CNV formation after laser-induced photocoagulation. Another study conducted by Li et al.[47] demonstrated that silencing CEBPB inhibited retinal avascular and pericyte loss to further reduce retinal neovascularization in rats with oxygen-induced retinopathy by modulating VEGF expression. However, CEBPB binding the GLS1 promoter has not been previously investigated. In this work, we demonstrated that the -525/-535 and -1312/-1322 regions in the 2000 bp promoter sequence upstream of the GLS1 gene were most likely the potential binding sites for CEBPB using a ChIP assay in HRMECs. Furthermore, CEBPB was found to be a direct target of miR-376b-3p in HRMECs. The overexpression of CEBPB promoted proliferation, motility, survival and tube formation and partially abolished the effects of miR-376b-3p in HRMECs. This finding indicates that CEBPB is highly likely the link we are searching for between miR-376b-3p and GLS1.

CONCLUSION

In summary, the present study demonstrated that miR-376b-3p inhibits proliferation, migration, and angiogenesis by suppressing GLS1-mediated glutaminolysis by targeting CEBPB in ECs. These findings shed new light on our understanding of the molecular regulatory network in CNV-related diseases and could provide potential therapeutic targets in the future.

References

1. Spaide RF. Choroidal neovascularization in younger patients. *Curr Opin Ophthalmol*. 1999;10:177–181.
2. Green WR, Wilson DJ. Choroidal neovascularization. *Ophthalmology*. 1986;93:1169–1176.
3. Wong CW, Yanagi Y, Lee WK, et al. Age-related macular degeneration and polypoidal choroidal vasculopathy in Asians. *Prog Retin Eye Res*. 2016;53:107–139.
4. Ohno-Matsui K, Ikuno Y, Lai T, Gemmy CC. Diagnosis and treatment guideline for myopic choroidal neovascularization due to pathologic myopia. *Prog Retin Eye Res*. 2018;63:92–106.
5. Campochiaro PA. Molecular pathogenesis of retinal and choroidal vascular diseases. *Prog Retin Eye Res*. 2015;49:67–81.
6. Saint-Geniez M, D'Amore PA. Development and pathology of the hyaloid, choroidal and retinal vasculature. *Int J Dev Biol*. 2004;48:1045–1058.
7. Mettu PS, Allingham MJ, Cousins SW. Incomplete response to Anti-VEGF therapy in neovascular AMD: Exploring

disease mechanisms and therapeutic opportunities. *Prog Retin Eye Res*. 2021;82:100906.

8. Jian L, Panpan Y, Wen X. Current choroidal neovascularization treatment. *Ophthalmologica*. 2013;230:55–61.

9. Potente M, Carmeliet P. The link between angiogenesis and endothelial metabolism. *Annu Rev Physiol*. 2017;79:43–66.

10. Eelen G, de Zeeuw P, Simons M, Carmeliet P. Endothelial cell metabolism in normal and diseased vasculature. *Circ Res*. 2015;116:1231–1244.

11. De Bock K, Georgiadou M, Schoors S, et al. Role of PFKFB3-driven glycolysis in vessel sprouting. *Cell*. 2013;154:651–663.

12. Peyton KJ, Liu XM, Yu Y, et al. Glutaminase-1 stimulates the proliferation, migration, and survival of human endothelial cells. *Biochem Pharmacol*. 2018;156:204–214.

13. Eelen G, Dubois C, Cantelmo AR, et al. Role of glutamine synthetase in angiogenesis beyond glutamine synthesis. *Nature*. 2018;561:63–69.

14. Kim B, Li J, Jang C, Arany Z. Glutamine fuels proliferation but not migration of endothelial cells. *EMBO J*. 2017;36:2321–2333.

15. Huang H, Vandekeere S, Kalucka J, et al. Role of glutamine and interlinked asparagine metabolism in vessel formation. *EMBO J*. 2017;36:2334–2352.

16. Lagos-Quintana M, Rauhut R, Lendeckel W, Tuschl T. Identification of novel genes coding for small expressed RNAs. *Science*. 2001;294:853–858.

17. Ambros V. microRNAs: tiny regulators with great potential. *Cell*. 2001;107:823–826.

18. Liu CH, Huang S, Britton WR, Chen J. MicroRNAs in Vascular Eye Diseases. *Int J Mol Sci*. 2020;21:649.

19. Zhang L, Liu S, Wang JH, et al. Differential Expressions of microRNAs and Transfer RNA-derived Small RNAs: Potential Targets of Choroidal Neovascularization. *Curr Eye Res*. 2019;44:1226–1235.

20. Zhang Y, Cai S, Jia Y, et al. Decoding Noncoding RNAs: Role of MicroRNAs and Long Noncoding RNAs in Ocular Neovascularization. *Theranostics*. 2017;7:3155–3167.

21. Feng Y, Wang J, Yuan Y, et al. miR-539-5p inhibits experimental choroidal neovascularization by targeting CXCR7. *FASEB J*. 2018;32:1626–1639.

22. Li LJ, Huang Q, Zhang N, et al. miR-376b-5p regulates angiogenesis in cerebral ischemia. *Mol Med Rep*. 2014;10:527–535.

23. Livak KJ, Schmittgen TD. Analysis of relative gene expression data using real-time quantitative PCR and the 2(-Delta Delta C(T)) Method. *Methods*. 2001;25:402–408.

24. Feng Y, Zou R, Zhang X, et al. YAP promotes ocular neovascularization by modifying PFKFB3-driven endothelial glycolysis. *Angiogenesis*. 2021;24:489–504.

25. Laferriere CA, Pang DS. Review of intraperitoneal injection of sodium pentobarbital as a method of euthanasia in laboratory rodents. *J Am Assoc Lab Anim Sci*. 2020;59:254–263.

26. Takehana Y, Kurokawa T, Kitamura T, et al. Suppression of laser-induced choroidal neovascularization by oral tranilast in the rat. *Invest Ophthalmol Vis Sci*. 1999;40:459–466.

27. Frankel D, Delecourt V, Novoa-Del-Toro EM, et al. miR-376a-3p and miR-376b-3p overexpression in Hutchinson-Gilford progeria fibroblasts inhibits cell proliferation and induces premature senescence. *iScience*. 2022;25:103757.

28. Kiezun A, Artzi S, Modai S, et al. miRviewer: a multispecies microRNA homologous viewer. *BMC Res Notes*. 2012;5:92.

29. Bharadwaj AS, Appukuttan B, Wilmarth PA, et al. Role of the retinal vascular endothelial cell in ocular disease. *Prog Retin Eye Res*. 2013;32:102–180.

30. Castro-Mondragon JA, Riudavets-Puig R, Rauluseviciute I, et al. JASPAR 2022: the 9th release of the open-access database of transcription factor binding profiles. *Nucleic Acids Res*. 2022;50:D165–D173.

31. Dreos R, Ambrosini G, Cavin PR, Bucher P. EPD and EPDnew, high-quality promoter resources in the next-generation sequencing era. *Nucleic Acids Res*. 2013;41:D157–D164.

32. McGeary SE, Lin KS, Shi CY, et al. The biochemical basis of microRNA targeting efficacy. *Science*. 2019;366:eaav1741.

33. Chen Y, Wang X. miRDB: an online database for prediction of functional microRNA targets. *Nucleic Acids Res*. 2020;48:D127–D131.

34. Das A, McGuire PG. Retinal and choroidal angiogenesis: pathophysiology and strategies for inhibition. *Prog Retin Eye Res*. 2003;22:721–748.

35. Zhang L, Yao M, Ma W, et al. MicroRNA-376b-3p targets RGS1 mRNA to inhibit proliferation, metastasis, and apoptosis in osteosarcoma. *Ann Transl Med*. 2021;9:1652.

36. Liu XW, Zhang CC, Zhang T. MiR-376b-3p functions as a tumor suppressor by targeting KLF15 in non-small cell lung cancer. *Eur Rev Med Pharmacol Sci*. 2020;24:9480–9486.

37. Dong MM, Peng SJ, Yuan YN, Luo HP. LncRNA TTN-AS1 contributes to gastric cancer progression by acting as a competing endogenous RNA of miR-376b-3p. *Neoplasma*. 2019;66:564–575.

38. Chen LM, Niu YD, Xiao M, et al. LncRNA NEAT1 regulated cell proliferation, invasion, migration and apoptosis by targeting has-miR-376b-3p/SULF1 axis in non-small cell lung cancer. *Eur Rev Med Pharmacol Sci*. 2020;24:4810–4821.

39. Li H, Xue Y, Ma J, et al. SNHG1 promotes malignant biological behaviors of glioma cells via microRNA-154-5p/miR-376b-3p- FOXP2- KDM5B participating positive feedback loop. *J Exp Clin Cancer Res*. 2019;38:59.

40. Eelen G, de Zeeuw P, Treps L, et al. Endothelial cell metabolism. *Physiol Rev*. 2018;98:3–58.

41. Unterluggauer H, Mazurek S, Lener B, et al. Premature senescence of human endothelial cells induced by inhibition of glutaminase. *Biogerontology*. 2008;9:247–259.

42. Feng Y, Yang X, Huang J, et al. Pharmacological Inhibition of glutaminase 1 attenuates alkali-induced corneal neovascularization by modulating macrophages. *Oxid Med Cell Longev*. 2022;2022:1106313.

43. Ramji DP, Foka P. CCAAT/enhancer-binding proteins: structure, function and regulation. *Biochem J*. 2002;365:561–575.

44. van der Krieken SE, Popeijus HE, Mensink RP, Plat J. CCAAT/enhancer binding protein beta in relation to ER stress, inflammation, and metabolic disturbances. *Biomed Res Int*. 2015;2015:324815.

45. Guo L, Li X, Tang QQ. Transcriptional regulation of adipocyte differentiation: a central role for CCAAT/enhancer-binding protein (C/EBP) beta. *J Biol Chem*. 2015;290:755–761.

46. Zhang P, Wang H, Luo X, et al. MicroRNA-155 inhibits polarization of macrophages to M2-type and suppresses choroidal neovascularization. *Inflammation*. 2018;41:143–153.

47. Li T, Cai X, Wang X, et al. CCAAT/enhancer-binding protein beta mediates oxygen-induced retinal neovascularization via retinal vascular damage and vascular endothelial growth factor. *J Diabetes Res*. 2020;2020:2789209.